Uranium ions adsorption from acid leach liquor using acid cured phosphate rock: kinetic, equilibrium, and thermodynamic studies

Article *in* Separation Science and Technology · February 2019

DOI: 10.1080/01496395.2019.1574305

CITATIONS
17

READS
385

3 authors:

L. A. Yousef
Nuclear Materials Authority of Egypt
19 PUBLICATIONS **88** CITATIONS
SEE PROFILE

A.M.A. Morsy
N.M.A
23 PUBLICATIONS **333** CITATIONS
SEE PROFILE

Mohammed Hagag
Nuclear Materials Authority of Egypt
18 PUBLICATIONS **134** CITATIONS
SEE PROFILE

Separation Science and Technology

ISSN: 0149-6395 (Print) 1520-5754 (Online) Journal homepage: https://www.tandfonline.com/loi/lsst20

Uranium ions adsorption from acid leach liquor using acid cured phosphate rock: kinetic, equilibrium, and thermodynamic studies

L. A. Yousef, A. M. A. Morsy & M. S. Hagag

To cite this article: L. A. Yousef, A. M. A. Morsy & M. S. Hagag (2019): Uranium ions adsorption from acid leach liquor using acid cured phosphate rock: kinetic, equilibrium, and thermodynamic studies, Separation Science and Technology, DOI: 10.1080/01496395.2019.1574305

To link to this article: https://doi.org/10.1080/01496395.2019.1574305

SEPARATION SCIENCE AND TECHNOLOGY
https://doi.org/10.1080/01496395.2019.1574305

Taylor & Francis
Taylor & Francis Group

Uranium ions adsorption from acid leach liquor using acid cured phosphate rock: kinetic, equilibrium, and thermodynamic studies

L. A. Yousef, A. M. A. Morsy, and M. S. Hagag

Nuclear Materials Authority, Cairo, Egypt

ABSTRACT

The adsorption of uranium from acid leach liquor was studied in batch experiments using acid cured phosphate rock (ACPR). Different factors affecting the adsorption process such as pH, contact time, L/S ratio, initial uranium concentration, and temperatures were investigated to optimize the operation conditions for the composite. The kinetic, equilibrium and thermodynamic characteristics of U (VI) adsorption using acid cured phosphate rock have been determined. Batch sorption experiments are performed to evaluate the optimum conditions at pH 4, L/S ratio (0.2) for 60 min. contact time at room temperature. The maximum sorption capacity from Langmuir reaches to 125 mg/g at room temperature. The kinetics data are well described by the pseudo-second-order kinetic model at 500 mg/L uranium concentration. The evaluation of thermodynamic parameters (ΔG^{o}, ΔH^{o} and ΔS^{o}) indicated that the adsorption process is spontaneous in nature, exothermic and randomness. Uranium (VI) can be desorbed from the loaded acid cured phosphate rock using 0.5M H_2SO_4 solution. Finally, the optimized factors have been carried out for uranium (VI) adsorption from Hammamat sediments leach liquor.

ARTICLE HISTORY
Received 19 September 2018
Accepted 22 January 2019

KEYWORDS
Phosphate rock; acid cured; uranium ions; adsorption; thermodynamics and kinetic studies

Introduction

Removal of toxic radioactive metal contaminants from waste effluents is a vital environmental issue. Several procedures are applied for removing the contaminant ions from the waste solutions *e.g.* chemical precipitation, ion exchange, reverses osmosis and solvent extraction.[1] However, using of these methods usually displays some disadvantages like; incomplete metal removal, high reagent and energy requirements, generation of toxic sludge or other waste products that require safe disposal.

On the other hand, using the adsorption technique for contaminants removal showed many advantages such as; easily-operability, low costs and high efficiency.[2,3] Several adsorbents have been recently used to remove contaminant ions such as; goethite, briniest[4], wool,[5] activated sludge,[6] iron oxide coated sand,[7] and zeolite silica[8] and composite and polymers.[9] Among them phosphates have shown high efficiency in removal of heavy metals and especially uranium from wastes.[10–12]

Phosphate ore contains calcium phosphate, silica, potassium, iron, aluminum, magnesium, organic matter, carbonates, and clay matter.[13] Most of the phosphate ores are consumed in the production of phosphates fertilizer, but few would be characterized by a high cost of phosphates fertilizer production, may serve as an adsorbent for many heavy metals.[14]

Several studies demonstrated that the existing active sites in phosphate rock results in efficient removal ability to pollutants.[15] Uranium (VI) phosphates has the lowest solubility over a broad range of conditions.[16] The low solubility of uranium (VI) phosphates suggest that phosphate materials may be useful for uranium (VI) adsorption, formation of uranyl phosphates.[17] Uranium removal via adsorption on phosphate solids has also been evaluated after addition of phosphate amendments to groundwater.[18]

The efficiency of the adsorption of uranium using phosphate rock less than in the case of the use of acid cured phosphate. This is attributed to the acid-treated phosphates transformation all cations found in phosphate rock into aluminum sulfate and some sulfate salts. This is reason for increasing the efficiency of adsorption.[19,20] Many papers have reported the sorption of heavy metals onto sulfate salts.[21,22]

Different mechanisms for metal removal by phosphate minerals have been mentioned in the literature : (1) ion exchange processes at the surface of PR[23] (2) surface complexation[24] (3) precipitation of some amorphous to poorly crystalline, mixed metal phosphates[25] and (4) substitution of Ca in PR by other metals during

CONTACT M. S. Hagag mohammedsobbhy@yahoo.com Nuclear Materials Authority, 530 El Maadi, Cairo, Egypt

re-crystallization (co precipitation).[26] Each mechanism can work solely or mixed with the other for metal removal.

In this study, uranium removal from aqueous solutions was investigated using an acid cured phosphate rock (ACPR). The effect of various parameters affecting sorption behavior such as contact time, pH and concentration of initial uranium ions were determined, also data of sorption isotherms, kinetics and thermodynamics were estimated. In addition, infrared spectrum (FTIR) was verified for characterization of phosphate rock, acid cured phosphate rock and after adsorption of uranium.

Materials and methods

Chemicals and reagents

The used chemicals of analytical grade were purchased from Merck Co. Deionized water was used in all experiment steps. The stock solution of U (VI) was prepared by dissolving exact amounts of $UO_2(NO_3)_2$.$6H_2O$ in concentrated nitric acid solution to avoid the hydrolysis of U (VI). The uranium concentration in aqueous phases was determined with Arsenazo III.[27] The absorbance of the formed uranium Arsenazo III complex was measured at 655 nm against proper standard solutions.

Phosphate rock

The used Egyptian phosphate was sampled from Abu Tartour plateau.[28] The chemical composition of the phosphate sample is given in Table 1. The major oxides SiO_2, Al_2O_3, P_2O_5 were analyzed using the spectrophotometer method. The content of Na_2O and K_2O were estimated by the flame photometric technique. Total Fe_2O_3, MgO and CaO percent were determined by titration method. The loss on ignition (L.O.I) was determined gravimetrically.[29] The estimated error for the major constituents was less than ±2%. Some trace elements such as Cr, Zr, Ni, Zn, and Ba were determined using atomic adsorption spectrometer device.

Table 1. Chemical composition of the phosphate rock.

Major oxides	Wt %
SiO_2	5.1
Al_2O_3	6.1
TiO_2	1.5
Fe_2O_3	3.9
CaO	41.6
MgO	2.9
Na_2O	2.4
K_2O	0.405
P_2O_5	25.6
L.O.I	10.2
Micro component	**(ppm)**
Zr	595
Cr	54
Ni	44
Zn	34
Ba	456

Preparation of (ACPR)

The collected technological sample of the phosphate rock was milled to −150 mesh. Phosphate ore was treated using sulfuric acid and nitric at 110°C for a period of 2 h where acid is added gradually. For every 100 grams of phosphate ore, 60 grams of sulfuric acid and 6.5 gm of nitric acid are adding with continuous stirring, The phosphate percentage in ACPR was not affected after the acid cured process (25.6%). Chemical analysis of phosphate ore before and after treatment did not change for cations only.

Uranium leach liquor

A stock leach liquor of the El Hammamat sediments (Gabal Gattar area, North Eastern Desert) was prepared under optimum leaching conditions,[30] except that nitric acid was taken instead of sulfuric acid that it verifies uranium leaching efficiency (70%). Analysis of the leach liquor obtained showed that it contained 2000 mg/L uranium. The chemical composition of the working El Hammamat sample is given in Table 2.

Instrumentation

Generally, the samples used in the work were weighted using analytical balance produced by Shimadzu (Ay 220) with a stability of sensitivity ±2 mg/L/C. UV-Visible spectrophotometer model "Metertech Inc" Sp 8001, was used for measuring (SiO_2, Al_2O_3, and P_2O_5). The UV visible ranges between 200 and 1100 nm with a wave length accuracy of ±1 nm. A portable digital meter equipped with a combined glass electrode with the standard ground joint was used for pH measurement using buffer solution of known values (4, 7, and 10) for calibration the pH meter.

Table 2. Chemical composition of El Hammamat sediments.

Component	Content, wt %	Component	Content, ppm
SiO_2	68.31	Cr	57
Al_2O_3	15.46	Co	10
Fe_2O_3	6.11	Zr	203
MgO	0.80	Ni	41
CaO	1.56	Cu	33
Na_2O	2.32	Zn	501
K_2O	3.60	Y	812
TiO_2	0.08	Ba	346
P_2O_5	0.31	Pb	383
MnO	0.07	Hf	11
L.O.I	1.20	Nb	177
		U	2850

Materials characterization

The prepared ACPR before and after uranium adsorption were characterized using Fourier Transform Infrared Spectrometer (FTIR) model Thermo Scientific Nicolet IS10, Germany.

Adsorption experiments

The uranium adsorption experiments were performed in beaker, where about 0.1g from the used acid cured phosphate rock was stirred with 20 mL of $UO_2(NO_3)_2.6H_2O$ solutions. The effect of several factors on the adsorption process were investigated where each factor was solely studied, while all other factors were kept constant. The applied factors were pH (in the range 1–7), contact time (0 to – 90 min), L/S (0.1 : 0.5), initial U (VI) concentration (50–1000, mg/L) and temperature (298–328 °K).

In each experiment, solution pH was adjusted using 0.1 M HCl and/or 0.1 M NaOH. The beakers were gently shaken and the samples were obtained at different time intervals. The mixture was centrifuged and filtered then uranium ions were determined spectrophotometrically in the filtrate. The adsorption capacity (qe) and removal efficiency were obtained using Eqs. (1) and (2):

$$qe\ (mg/g) = (C_o - C_e) * V/m \quad (1)$$

$$\text{Removal efficiency}\ (\%) = [(C_o - C_e)/C_o] * 100 \quad (2)$$

where C_o and C_e are the U (VI) ions concentration in the initial solution and at equilibrium (mg/L) respectively, V is the volume of the solution (L), m is the weight of adsorbent (g) and qe is the amount of U (VI) adsorbed on the used acid cured phosphate rock at equilibrium.

Results and discussion

Batch experiments

Impact of contact time

The uranium (VI) sorption on to the ACPR increased with increasing of the contact time and reached its maximum value of adsorption at 60 min (98%). More contact time did not reveal any significant increasing for U (VI) sorption (Fig. 1). The adsorption kinetics involves two phases (i) first a rapid uptake of the metal due to presence of an initial mass driving force (ii) second phase corresponds to the slow increase of metal uptake.

Kinetics of sorption process

To verify the kinetics of uranium sorption, the obtained data were tested by pseudo-first-order (eq.3) and pseudo-first-order (eq.4).

$$Log(q_e - q_t) = logq_e - (K_1/2.303)t \quad (3)$$

$$\left(\frac{t}{qt}\right) = \frac{1}{k_2 q_e^2} + \frac{1}{q_e}(t) \quad (4)$$

where q_e and q_t are the sorption capacities at equilibrium and at time *t*, respectively, and k_1 is the pseudo-first-order rate constant (min^{-1}), and the pseudo-second-order sorption (k_2).

The values of q_{cal}, q_{exp} and R^2 of both the applied models are listed in Table.3 Based on these values, it is clear that the uranium sorption process follows the

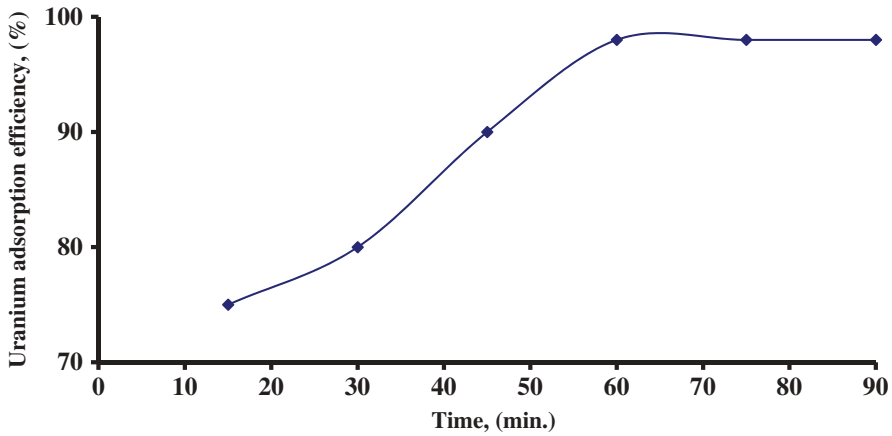

Figure 1. Impact of contact time on uranium adsorption by ACPR.
Adsorption conditions: room temp., 500 ppm U concentration, pH 4 and L/S ratio 0.2

Table 3. Calculated parameters of the kinetic models with the linear correlation coefficients (R^2) of each plot.

Kinetic models	Parameters		Straight line Equation
Pseudo first order	$K_1(min^{-1})$	0.1	**Y = – 0.0437X +2.3571**
	q_{cal}	227.56	
	q_{exp}	95	
	R^2	0.86	
Pseudo second order	K_2(g/(mg. min)	0.001118	**Y = 0.0092x+0.0757**
	q_{cal}	108.69	
	q_{exp}	95	
	R^2	0.99	

pseudo second-order model that supports the chemisorption nature of this process. This observation further proves the higher sorption capacity of used adsorbent as compares to the other adsorbent.[31–34]

Impact of L/S ratio

The achieved results (Fig. 2) point to proportional increasing between the L/S ratio and uranium adsorption percentage. The maximum adsorption was obtained at L/S ratio (0.2). Further increasing of the L/S was accompanied by stability of U-adsorption. This may be back to the vacant space has been saturated with the uranium ions. Similar result was obtained for thorium sorption on magnetic talc titanium oxide.[35]

Impact of pH

One of the most important parameters in the adsorption experiments of metal ions from solutions is the pH of the medium. The obtained results from this experimental (Fig. 3) showed that the maximum sorption capacity for uranium ions was achieved at pH value 4 while it decreased with the further elevation of pH. The sorption behavior with pH variation should be interpreted in successive steps. The first step includes the low sorption capacity with the low pH values (< 3) which is reasonably attributed to protonation of sorbent surface that causes an electrostatic repulsive force with the U (VI) ions. The second step involved increasing of U-sorption with increasing the pH to 3 and reached its maximum sorption capacity at pH = 4 which is likely understood when we consider decreasing of +ve charges onto sorbent surface enhancing of U (VI) ions to be sorped on the used sorbent. The third step represents the sorption behavior with pH >4 where

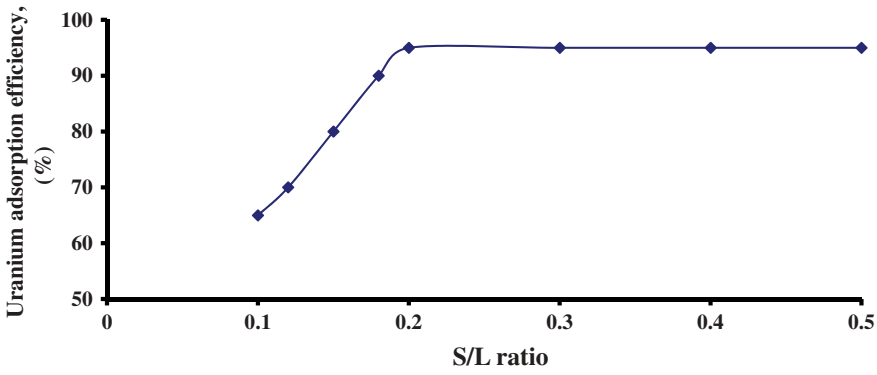

Figure 2. Impact of uranium volume (ml) on uranium sorption on ACPR.
Adsorption conditions pH 4, room temp., 500 ppm U (VI) ions concentration, 0.1 g of resin, 60 min.

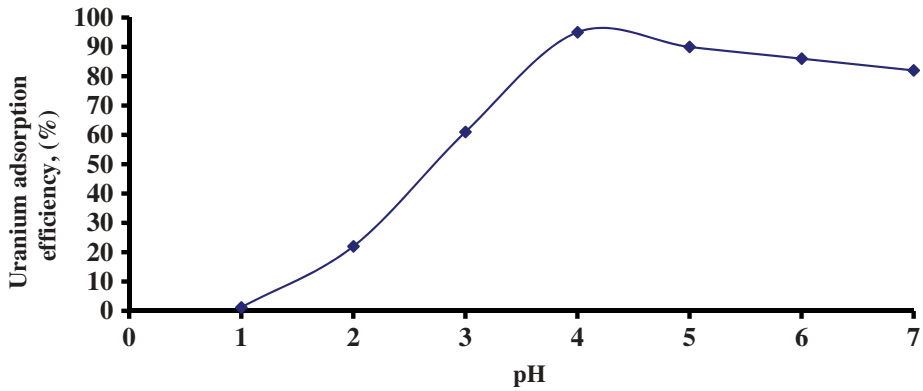

Figure 3. Impact of initial pH on uranium adsorption by ACPR.
Adsorption conditions U concentration 500 mg/L, room temp., L/S ratio 0.2 and contact time 60 min.

gradual decreasing of U-sorption was observed which is expected due to the dominant of the negatively charged U-species as well as the formed – ve charges on the sorbent surface. Similar results was obtained for lead sorption on phosphate rock[36,37] stated that the adsorption isotherm of Pb (II), Cu (II), and Zn (II) onto calcined phosphate was obtained at pH 5. These results are in good agreement with the results of sorption of Zn^{2+} and Cd^{2+}on hydroxyl-apatite surfaces.[38] The aqueous speciation distribution of uranium was calculated and represented in Fig. 4. The results showed that the complexes of $UO_2NO_3^+$ are the predominant species at the pH range from 0.0 to 4 with mean total percent of 91%. U-hydroxide complexes start to dominate the aqueous phase at pH after 4. The dominate complex of UO_2 $(OH)_2.H_2O$ became the major specie with about 100% of total concentration at pH range from 5 to 11. After pH 12, UO_2 $(OH)_4^{2-}$ and UO_2 $(OH)_3^-$ became the major species. According to the initial pH of 4–6.5, the following adsorption scheme is more appropriate to be considered and the possible coordination mechanism for the interaction between $UO_2NO_3^+$and ACPR adsorbent is followed:

$$(ACRP)OH^- + UO_2NO_3^+ \rightarrow (ACRP)\ OH.UO_2NO_3$$

Impact of initial uranium concentration

The obtained results (Fig. 5) revealed that the adsorption percent was nearly stable (≈98.5% efficiency), as initial U concentration increased from 50

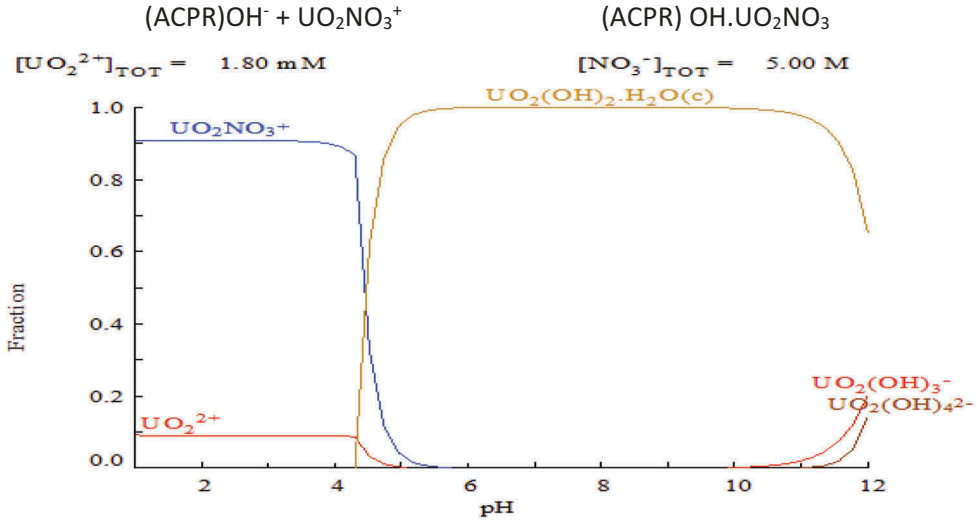

Figure 4. Expected aqueous speciation of uranium (500 mg/L) of pH in 5 M HNO_3 using Medusa and Hydra program.[30]

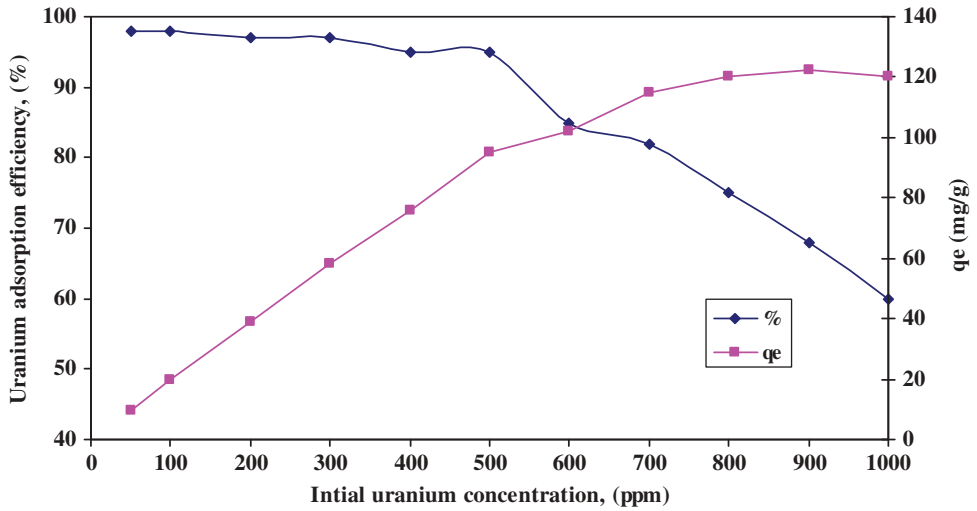

Figure 5. Impact of initial uranium concentration on uranium adsorption by ACPR.
Adsorption conditions: pH 4, room temp., L/S ratio 0.2 and contact time 60 min.

to 100 mg/L. Then with increasing of the initial U concentration, the efficiency decreased but on the contrary the amount of adsorbed uranium (qe) increased. This may be back to the limited number of active sites present on the adsorbent, which will become saturated at a certain concentration. With the increase in the uranium concentration, uranium ions will compete for the available functions groups on the surface of adsorbent material, the matter that will lead to decrease in the adsorption percent.[34,39] While, the adsorption of (PR) without acid cured was (49%) indicating that the acid cured process had highly efficient on uranium adsorption.

Sorption isotherms

Langmuir adsorption isotherm

Langmuir adsorption isotherm is valid for monolayer adsorption onto a surface containing a finite number of identical sites. The model assumes uniform energies of adsorption onto the surface and no transmigration of adsorbate in the plane of the surface.

Freundlich adsorption isotherm commonly describes the adsorption characteristics for the heterogeneous surface. The linear form of Langmuir and Freundlich isotherms are presented by Eqs. (5) and (6) respectively[40]:

$$\frac{C_e}{q_e} = \frac{1}{bq_{\max}} + \frac{C_e}{q_{\max}} \tag{5}$$

$$\ln q_e = \ln K_F + \frac{1}{n} \ln C_e \tag{6}$$

where C_e is the equilibrium concentration of uranium in the solution (mg/L), q_e is the amount of uranium adsorbed per weight unit of ACPR at equilibrium time (mg/g), q_{max} is the saturated monolayer adsorption capacity (mg/g) and b is the Langmuir constant (L/mg), K_F (mg/g), 1/n (L/mg) and n are the freundlich constants related to the adsorption capacity and adsorption intensity, respectively.

The obtained results of the uranium adsorption isotherms Table 4 correlate better with the langmuir isotherm than freundlich isotherms where the maximum adsorption value obtained in accordance to Langmuir is 125 mg/g. It also indicates that the uptake occurred on a homogeneous surface by monolayer adsorption and all metal binding sites are energetically the same.[41,42]

One of the essential characteristics of the Langmuir model could be expressed by dimensionless constant called equilibrium parameter R_L, that describes the favorability of the adsorption process [43]:

$$R_L = 1/1 + b\ Co$$

where C_0 is the highest initial metal ion concentration (mg/L). The value of R_L indicates the type of isotherm to be irreversible ($R_L = 0$), favorable ($0 < RL < 1$), linear ($RL = 1$), or unfavorable ($RL > 1$). RL value (Table 4) was found to be less than 1 and greater than 0 indicating the favorable sorption isotherm of uranium ions.

Table 4. Langmuir and Freundlich isotherm constants for uranium ions adsorption onto ACPR.

Langmuir pararmeters		Freunlich pararmeters	
$q_{max}(mgg^{-1})$	125	K_f (mg g^{-1})	17.35
B (Lmg^{-1})	0.085	1/n	0.382
R^2	0.99	R^2	0.85
equation	y = 0.008x + 0.0931	equation	y = 0.3826x + 1.2393

Impact of temperature

The effect of temperature on the adsorption efficiency of ACPR toward uranyl ions from aqueous solutions (Fig. 6) indicates that ACPR has better adsorption ability at low temperature (298 °K) while a clear decreasing was manifested with the temperature increasing. This mainly depends on the physical adsorption nature and nature of the chelating groups in the ACPR matrix. It can be assumed that the bond between the phosphate group and uranium ions may be broken down.[44]

Thermodynamic

Thermodynamic parameters including enthalpy change ($\Delta H°$), Gibbs free energy change ($\Delta G°$) and entropy change ($\Delta S°$) can be estimated by using equilibrium constants changing with temperature. According to thermodynamics, the distribution coefficient is related to the enthalpy change (($\Delta H°$) and entropy change ($\Delta S°$) at constant temperature by the following equation:

$$\log K_d = -\frac{\Delta H^\circ}{2.303\ R} \cdot \frac{1}{T} C \tag{7}$$

$$-\Delta G = 2.303\ RT \log K\ d \tag{8}$$

where $\log K_d$ is the distribution coefficient ($cm^3\ g^{-1}$), $\Delta S°$ is standard entropy, $\Delta H°$ is standard enthalpy, T is the absolute temperature (K), R is gas constant (kJ $mol^{-1}\ K^{-1}$). The standard free energy values were calculated from:

$$\Delta G^\circ = \Delta H^\circ - T\Delta S^\circ \tag{9}$$

The values of enthalpy change ($\Delta H°$) and entropy change ($\Delta S°$) are calculated from the slope and intercept of the plot of log (K_d) versus (1/T). The negative value of $\Delta H°$ (−44.71 KJ/mol) indicates that the

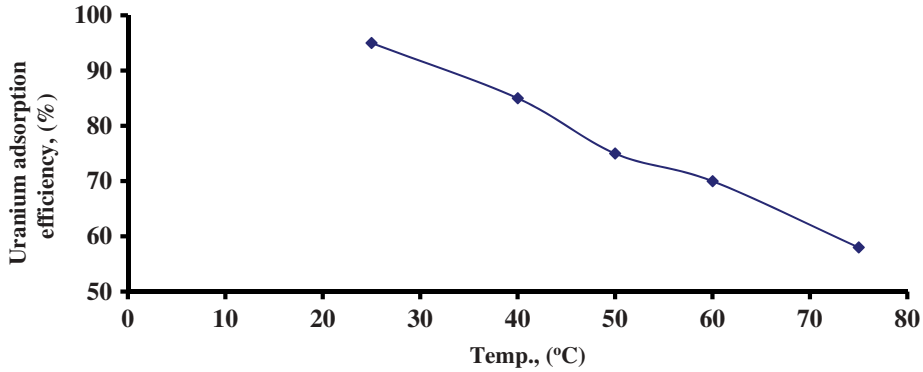

Figure 6. Impact of temperature on uranium adsorption by ACPR.
Adsorption conditions pH 4, room temp., L/S ratio 0.2 and contact time 60 min.

Table 5. Thermodynamic parameters for the uranium adsorption onto the ACPR.

Temperature, (°K)	(ΔH^o) KJ/mol	(ΔG^o) KJ/mol	(ΔS^o) KJ/mol K^{1-}
298	−44.71	−3.30	−0.1389

adsorption of uranium on the ACRP is exothermic. In addition, the negative standard free energy ΔG° (−3.30 KJ/mol), the reaction is spontaneous. The negative standard entropy ΔS° (−0.1389 KJ/mol K^{1-}) indicated that the adsorption, also all thermodynamics parameter was stated in Table 5.

Impact of eluting agents

To select the best eluting agent, different concentrations of three mineral acids ranging from 0.25 to 3 M were examined as eluting agents at room temperature using 20 ml acid volume on 0.1 g loaded acid cured phosphate rock for 60 min. at room temperature. The elution efficiency has been attained 99% with 20 ml of 0.5M H_2SO_4, 2M HCl or 2M HNO_3 acid solution from 0.1g loaded resin.

Case study

From the above results, (ACPR) has been used to extract the uranium from the acid leach liquor of Hammamat sediments (assaying 2000 mg/L U). The applied experiment has been achieved under optimum conditions pH 4, 60 min contact time, at room temperature by mixing 4L of the leach liquor with 20 g of (ACPR). The obtained results revealed an adsorption efficiency equals 95%. On the other hand, the loaded uranium has eluted using 100 ml of 0.5M sulfuric acid. The eluted uranium was precipitated using hydrogen peroxide at pH 2 and uranium is precipitated as 2.05g (UO_4. $2H_2O$). The uranium content in the uranium concentrate produced is 63% attaining a purity of 88.7%.

FTIR characterization of PR, ACPR and after adsorption of uranium

In order to determine the responsible function groups, the FTIR spectra of PR, ACPR and after adsorption of uranium onto ACPR were performed that are given in (Fig. 7). The chart of phosphate rock (PR), 1113 and 1040 cm^{-1} peaks represented P=O stretch. Also, at 2522–2002 cm^{-1} represented O=P-OH broad bands involving OH stretch from. The broad bands at 3534 and 3404 cm^{-1} corresponding to the stretching vibration of the lattice OH ions in PR.[45] The vibration broad bands at 1624–1429 cm^{-1} are related to the H_2O band and stretching vibration of PO_2.[46] The characteristic bands of the tetrahedron PO_4^{3-} in PR appear at 446, 569, 601, and 930 cm^{-1} (asymmetric bending vibration) (Fig.7a). These bands were shifted to 467.1, 595.28, 614, and 998.96 cm^{-1} after acid curing. Acid cured phosphate rock (ACPR) has new peaks appears at 1156.98 and 959.99 cm^{-1}, (which is characteristics for sulfate group) and peak at 778.7 cm^{-1} this give indication for the present of sulfate group in phosphate rock after acidic curing (Fig. 7b). While, after uranium adsorption, the peaks at 1156.98, 959.99, and 569.59 cm^{-1} disappeared and new peaks appeared at 1683.78, 1867.04, and 2134.05 cm^{-1} which indicated the adsorption of uranium over acidic cured phosphate rock (Fig. 7c).

Table 6 References [47–51] give the comparison for uptake of different adsorbents toward uranium.

Conclusion

In the present study, phosphate rock was cured with acids and characterized. Analysis indicated that sulfate groups were present on the surface of ACPR providing

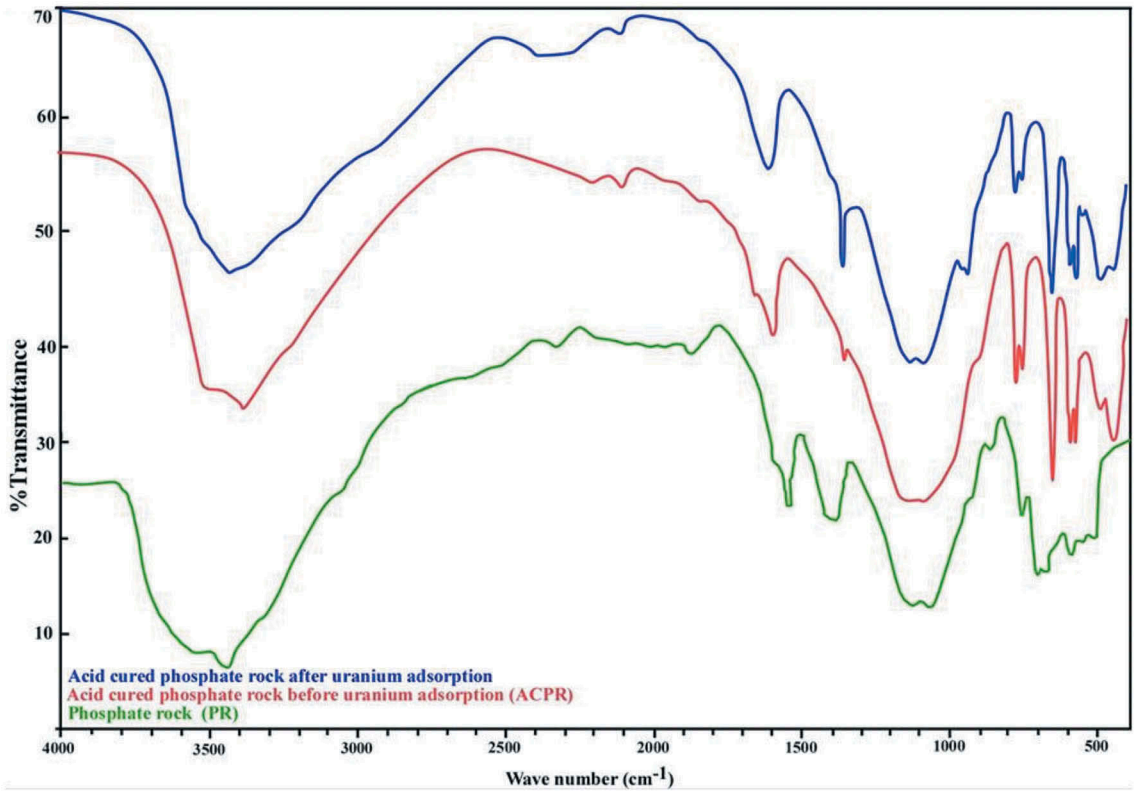

Figure 7. FTIR for the PR, ACPR and ACPR after uranium adsorption.

Table 6. Comparison for uptake of different adsorbents towards uranium.

Adsorbent	Uptake g/gm	Reference No.
Acid cured phosphate rock	125	This study
RHA–aluminum composite	85	34
chitosan modified phosphate rock	8.06	47
Phosphoryl functionalized mesoporous silica	199.6	48
Amidoxime modified multiwalled carbon	67.9	49
Phosphate rock apatite (PRA)	0.2021	50
Polypyrrole	87.72	51

a highly potential adsorption material for uranium ions. Indeed, the presence of sulfate groups showed greatly improved U (VI) uptake properties compared to original. Among the equilibrium isotherm models, the Langmuir model was in a good agreement with the experimental data with high correlation coefficient. Kinetic study showed that the pseudo-second-order model was appropriate to describe the adsorption process. Feasible improvements in the adsorptions properties along with the acid cured properties encourage the use of phosphate rock as uranium adsorbent materials.

ORCID

M. S. Hagag http://orcid.org/0000-0002-3591-836X

References

[1] Elouear, Z.; Bouzid, J.; Boujelben, A.; Feki, M.; Jamoussi, F.; Montiel, A. (2008) Heavy metal removal from aqueous solutions by activated phosphate rock. *Journal of hazardous materials*, 156 (1–3): 412–420. doi:10.1016/j.jhazmat.2007.12.036.

[2] Zareh, M.M.; Aldaher, A.; Hussein, A.E.M.; Mahfouz, M.G.; Soliman, M. (2012) Uranium adsorption from a liquid waste using thermally and chemically modified bentonite. *Journal of Radioanalalytical Nuclear Chemistry*, 295: 1153–1159. doi:10.1007/s10967-012-2234-8.

[3] Buerge-Weirich, D.; Hari, R.; Xue, H.; Behra, P.; Sigg, L. (2002) Adsorption of Cu,Cd and Ni ongoethite in the presence of natural groundwater ligands. *Environmental Science & Technology*, 36 (3): 328–336. doi:10.1021/es010892i.

[4] Manning, B.A.; Fendorf, S.E.; Bostick, B.; Suarez, D.L. (2002) Arsenic (III) oxidation and arsenic (V) adsorption reactions on synthetic birnessit. *Environmental Science & Technology*, 36: 976–981. doi:10.1021/es0110170.

[5] McNeil, S.;. (2001) Heavy metal removal using wool filters. *Asian Textile Journal*, 10: 88–90.doi:10.13140/2.1.5059.6480.

[6] Wang, X.J.; Xia, S.Q.; Cwen, L.; Zhao, J.F.; Chovelon, J. M.; Nicole, J.R. (2006) Bio-sorption of cadmium (II) and lead (II) ions from aqueous solutions onto dried activated sludge. *Journal of Environmental Sciences*, 247: 137–143. doi:10.1016/S1001-0742(06)60002-8.

[7] Benjamin, M.M.; Slatten, R.S.; Bailey, R.P.; Bennett, T. (1996) Sorption and filtration of metals using iron oxide coated sand. *Water Research*, 30: 2609–2620. doi:10.1016/S0043-1354(96)00161-3.

[8] Khalil, L.B.; Attia, A.A.; El-Nabarawy, T. (2011) Modified silica for the extraction of Cd(II), Cu(II) and Zn(II) ions from their aqueous solutions. *Adsorption Science & Technology*, 19: 511–523. doi:10.1260/0263617011494367.

[9] Say, R.D.; Senel, S.; Denizli, A. (2002) Preparation of cibacron blue f3ga-attached polyamide hollow fibers for heavy metal removal. *Journal of Applied Polymer Science*, 83: 3089–3098. doi:10.1002/app.2338.

[10] Minh, D.P.; Tran, N.D.; Nzihou, A.; Sharrock, P. (2014) Calcium phosphate based materials starting from calcium carbonate and orthophosphoric acid for the removal of lead(II) from an aqueous solution. *Chemical Engineering Journal*, 243: 280–288. doi:10.1016/j.cej.2014.01.032.

[11] Yuan, D.; Xiong, X.; Chen, L.; Lv, Y.; Wang, Y.; Yuan, L.; Liao, S.; Zhang, Q. (2016) Removal of uranium from aqueous solution by phosphate functionalized superparamagnetic polymer microspheres Fe3O4/P(GMA–AA–MMA). *Journal of Radioanalytical and Nuclear Chemistry*, 309 (2): 729–741. doi: 10.1007/s10967-015-4682-4.

[12] Kapnisti, M.; Noli, F.; Misaelides, P.; Vourlias, G.; Karfaridis, D.; Hatzidimitriou, A. (2018) Enhanced sorption capacities for lead and uranium using titanium phosphates; sorption, kinetics, equilibrium studies and mechanism implication. *Chemical Engineering Journal*, 342: 184–195. doi:10.1016/j.cej.2018.02.066.

[13] Abou El-Anwar, E.A.; Mekky, H.S.; Abd El Rahim, S. H.; Aita, S.K. (2017) Mineralogical, geochemical characteristics and origin of Late Cretaceous phosphorite in Duwi Formation (Geble Duwi Mine), Red Sea region, Egypt. *Egyptian Journal of Petroleum*, 26 (1): 157–169. doi:10.1016/j.ejpe.2016.01.004.

[14] De Gisi, S.; Lofrano, G.; Grassi, M.; Notarnicola, M. (2016) Characteristics and adsorption capacities of low-cost sorbents for wastewater treatment: A review. *Sustainable Materials and Technologies*, 9: 10–40. doi:10.1016/j.susmat.2016.06.002.

[15] Malash, G.F.; El-Khaiary, M.I. (2010) Methylene blue adsorption by the waste of Abu-Tartour phosphate rock. *Journal of Colloid and Interface Science*, 348 (2): 537–545. doi:10.1016/j.jcis.2010.05.005.

[16] Finch, R.; Murakami, T. (1999) Systematics and par agenesis of uranium mineral. *Reviews in Mineralogy and Geochemistry*, 38: 91–179. https://pubs.geoscienceworld.org/msa/rimg/article-abstract/38/1/91/87420/systematics-and-paragenesis-of-uranium-minerals?redirectedFrom=fulltext.

[17] Jerden, J.L.; Sinha, A.K.; Zelazny, L. (2003) Natural Immobilization of uranium by phosphate mineralization in an oxidizing saprolite-soil profile: chemical weathering of the Coles Hill Uranium deposit, Virgini. *Chemical Geology*, 199: 129–157. doi:10.1016/S0009-2541(03)00080-9.

[18] Fuller, C.C.; Bargar, J.R.; Davis, J.A.; Piana, M.J. (2002) Mechanisms of uranium interactions with hydroxyl apatite: implications for groundwater remediation. *Environmental Science & Technology*, 36: 158–165. doi:10.1021/es0108483.

[19] Geelhoed, J.S.; Hiemstra, T.; Van Riemsdijk, W.H. (1997) Phosphate and sulfate adsorption on goethite: single anion and competitive adsorption. *Geochimica Et Cosmochimica Act*, 61 (12): 2389–2396. doi:10.1016/S0016-7037(97)00096-3.

[20] Adebowale, K.O.; Unuabonah, I.E.; Olu-Owolabi, B.I. (2005) Adsorption of some heavy metal ions on sulfate- and phosphate-modified kaolin. *Applied Clay Science*, 29 (2): 145–148. doi:10.1016/j.clay.2004.10.003.

[21] Mohamed, E.E.; Elmetwaly, M.S.; Faiz, F.; Ali, I.I. (2014) The effect of chloride and sulfate ions on the adsorption of Cd^{2+} on clay and sandy loam Egyptian soils. *Scientific World Journal*, 1–6. doi:10.1155/2014/806252.

[22] Liu, J.; Zhu, R.; Liang, X.; Ma, L.; Lin, X.; Zhu, J.; He, H.; Parker, S.C.; Molinari, M. (2018) Synergistic adsorption of Cd(II) with sulfate/phosphate on ferrihydrite: an in situ ATR-FTIR/2D-COS study. *Chemical Geology*, 477: 12–21. doi:10.1016/j.chemgeo.2017.12.004.

[23] Middelburg, J.J.; Comans, R.N.J. (1991) Sorption of cadmium on hydroxyapatite. *Chemical Geology*, 90 (45–53). doi:10.1016/0009-2541(91)90032-M.

[24] Lin, R.; Chi, L.; Wang, Z.; Sui, Y.; Wang, Y.; Arandiyan, H. (2018) Review of metal (hydr)oxide and other adsorptive materials for phosphate removal from water. *Journal of Environmental Chemical Engineering*, 6 (4): 5269–5286. doi:10.1016/j.jece.2018.08.008.

[25] Ma, L.Q.; Logan, T.J.; Traina, S.J. (1995) Lead immobilization from aqueous solutions and contaminated soils using phosphate rocks. *Environmental Science & Technology*, 29: 1118–1126. doi:10.1021/es00004a034.

[26] Chen, X.; Wright, J.V.; Concha, J.L.; Peurrung, L.M. (1997) Effects of pH on heavy metal sorption on mineral apatite. *Environmental Science & Technology*, 31 (3): 624–631. doi:10.1021/es950882f.

[27] Marczenko, Z.;. (1976) *Spectrophotometric Determination of Elements*; Horwood: New York, 580p. ISBN 0470568658, 9780470568651

[28] El Nady, M.M.; Hammad, M.M. (2015) Organic richness, kerogen types and maturity in the shales of the Dakhla and Duwi formations in Abu Tartur area, Western Desert, Egypt: implication of Rock–eval pyrolysis. *Journal of Egyptian of Petrolum*, 24: 423–428. doi:10.1016/j.ejpe.2015.10.003.

[29] Shapiro, L.; Brannock, W.W. (1962) Rapid analysis of silicate, carbonate and phosphate rocks. *US. geological survey bulletin1401*, 1-144-A. https://pubs.usgs.gov/bul/1401/report.pdf

[30] Mahfous, M.G. (2004) Geochemistry and uranium-leaching characteristics of some younger granites—hammamat sediment contact zones at northern and central eastern desert. *PhD Thesis*; Ain Shams Univeristy: Egypt, 155p.

[31] Mouflih, M.; Aklil, A.; Jahroud, N.; Goura, M.; Sebtib, S. (2006) Removal of lead from aqueous solutions by natural phosphate. *Hydrometallurgy*, 81 (3–4): 219–225. doi:10.1016/j.hydromet.2005.12.011.

[32] Deihimi, N.; Irannajad, M.; Rezai, B. (2018) Equilibrium and kinetic studies of ferricyanide

adsorption from aqueous solution by activated red mud. *Journal of Environmental Management*, 227: 277–285. doi:10.1016/j.jenvman.2018.08.089.

[33] Jang, H.M.; Yoo, S.; Choi, Y.; Park, S.; Kan, E. (2018) Adsorption isotherm, kinetic modeling and mechanism of tetracycline on Pinus taeda-derived activated biochar. *Bioresource Technology*, 259: 24–31. doi:10.1016/j.biortech.2018.03.013.

[34] Youssef, W.M.; Hagag, M.S.; Ali, A.H. (2018) Synthesis, characterization and application of composite derived from rice husk ash with aluminium oxide for sorption of uranium. *Adsorption Science and Technology*, 36 (5–6): 1274–1293. doi:10.1177/2F0263617418768920.

[35] Morsy, A.M.A. (2017) Performance of magnetic talc titanium oxide composite for thorium ions adsorption from acidic solution. *Environmental Technology & Innovation*, 8: 399–410. doi:10.1016/j.eti.2017.09.004.

[36] Keles, E.; Kadir, A.; Yoruk, S. (2010) Removal of $Pb^{2+}$from aqueous solutions by rock phosphate (low-grade). *Desalination*, 253: 124–128. doi:10.1016/j.desal.2009.11.021.

[37] Aklil, A.; Mouflih, M.; Sebti, S. (2004) Removal of heavy metal ions from water by using calcined phosphate as a new adsorbent. *Journal of Hazardous Materials*, 112: 183–190. doi:10.1016/j.jhazmat.2004.05.018.

[38] Yuping, X.; Schwartz, F.; Traina, S.J. (1994) Sorption of Zn^{2+} and Cd^{2+} on hydroxyapatite surfaces. *Environmental Science & Technology*, 28: 1472–1480. doi:10.1021/es00057a015.

[39] Yang, R.T.;. (2003) Adsorbents: fundamentals and applications; John Wiley & Sons, Inc.: Canada. doi:10.1002/047144409X.

[40] Wang, C.; Boithias, L.; Ning, Z.; Han, Y.; Hatano, R. (2017) Comparison of Langmuir and Freundlich adsorption equations within the SWAT-K model for assessing potassium environmental losses at basin scale. *Agricultural Water Management*, 180B: 205–2011. doi:10.1016/j.agwat.2016.08.001.

[41] Tunali, S.; Akar, T. (2006) Zn (II) biosorption properties of Botrytis cinerea biomass. *Journal of Hazardous Materials*, 131 (1–3): 137–145. doi:10.1016/j.jhazmat.2005.09.024.

[42] Mohamed, S.; Karthikeyan, J. (1997) Removal of lignin and tannin color from aqueous solution by adsorption on to activated carbon solution by adsorption on to activated charcoal. *Environmental Pollution*, 97: 183–187. doi: 10.1016/S0269-7491(97)00025-0.

[43] Mohan, D.; Chander, S. (2006) Single, binary, and multi component sorption of iron and manganese on lignit. *Journal of Colloid and Interface Science*, 299: 57–76. doi: 10.1016/j.jcis.2006.02.010.

[44] Nyquist, R.A.; Craver, C.D. (1977) *The Coblentz Society Desk Book of Infrared Spectra*. In Craver, C.D.;editor; The Coblentz Society: French Village (MO), 399p.

[45] Veiderma, M.; Tõnsuaadu, K.; Knubovets, R.; Peld, M. (2005) Impact of anionic substitutions on apatite structure and properties. *Journal of Organometallic Chemistry*, 690 (10): 2638–2643. doi:10.1016/j.jorganchem.2004.11.022.

[46] Hammami, H.; El-Feki, H.; Marsan, O.; Drouet, C. (2016) Adsorption of nucleotides on biomimetic apatite: the case of adenosine Triphosphate (ATP). *Applied Surface Science*, 360: 979–988. doi:10.1016/j.apsusc.2015.11.100.

[47] Sun, Z.; Chen, D.; Chen, B.; Kong, L.; Su, M. (2018) Enhanced uranium(VI) adsorption by chitosan modified phosphate rock. *Colloids and Surfaces A: Physicochemical and Engineering Aspects*, 547: 141–147. doi:10.1016/j.colsurfa.2018.02.043.

[48] Guo, X.; Feng, Y.; Ma, L.; Gao, D.; Jing, J.; Yu, J.; Sun, H.; Gong, H.; Yujun Zhang, Y. (2017) Phosphoryl functionalized mesoporous silica for uranium adsorption. *Applied Surface Science*, 402: 53–60. doi:10.1016/j.apsusc.2017.01.050.

[49] Wu, J.; Tian, K.; Wang, J. (2018) Adsorption of uranium (VI) by amidoxime modified multiwalled carbon nanotubes. *Progress in Nuclear Energy*, 106: 79–86. doi:10.1016/j.pnucene.2018.02.020.

[50] Chen, B.; Wang, J.; Kong, L.; Mai, X.; Zheng, N.; Zhong, Q.; Liang, J.; Chen, D. (2017). Adsorption of uranium from uranium mine contaminated water using phosphate rock apatite (PRA): isotherm, kinetic and characterization studies. *Colloids and Surfaces A: Physicochemical and Engineering Aspects*, 520: 612–621. doi:10.1016/j.colsurfa.2017.01.055.

[51] Abdi, S.; Nasiri, M.; Mesbahi, A.; Khani, M.H. (2017) Investigation of uranium (VI) adsorption by polypyrrole. *Journal of Hazardous Materials*, 332: 132–139. doi:10.1016/j.jhazmat.2017.01.013.